DR. VALERIE L. WIESNER (Orcid ID : 0000-0001-9670-1394)

Article type : Article

Horizontal Dip-Spin Casting of Aqueous Alumina-Polyvinylpyrrolidone Suspensions with Chopped Fiber

V.L. Wiesner[a,*, ‡], M. Acosta[b, *, ‡, +], L.M. Rueschhoff[b, ‡], J.P. Youngblood[b], and R.W. Trice[b, †, ‡]

[a] NASA Glenn Research Center, Cleveland, OH 44135, U.S.A.

[b]Neil Armstrong Hall of Engineering, Purdue University School of Materials Engineering, 701 West Stadium Avenue, West Lafayette, IN 47907, U.S.A.

Abstract

A novel ceramic processing method, called Horizontal Dip Spin Casting (HDSC), enabled fabrication of tubular ceramic parts with an aligned chopped fiber phase. HDSC was demonstrated using highly loaded aqueous alumina suspensions with >50 vol.% solids loading and ≤5 vol.% water-soluble polymer employed as a rheological modifier. Chopped carbon fibers were added to the suspensions to attain maximum loadings of 30 vol.%. During forming, cylindrical foam molds were dipped into the suspension while being rotated radially about the long axis. Simultaneously, a doctor blade was placed at a specified distance from the foam surface to facilitate the flow of the suspension to align the fiber and control the thickness of the material that accrued on the mold. Rheological study of alumina-PVP suspensions with and without chopped carbon fiber showed that the suspensions exhibited a

This article has been accepted for publication and undergone full peer review but has not been through the copyediting, typesetting, pagination and proofreading process, which may lead to differences between this version and the Version of Record. Please cite this article as doi: 10.1111/ijac.12714

yield-pseudoplastic flow behavior. The degree of alignment of the carbon fiber phase in the green bodies was characterized for various suspension formulations, carbon fiber contents and forming speeds. Stereological characterization of green body specimens confirmed the effectiveness of HDSC to attain the desired tubular geometry with considerable fiber alignment for a suspension composition containing ≤20 vol.% chopped fibers.

Keywords: Ceramic processing, colloidal processing, alumina, fiber alignment, ceramic composites

1. Introduction

Ceramics are an attractive material system for use in numerous engineering fields due to their exceptional strength, hardness, corrosion and wear resistance at high temperatures. Despite their unique properties, monolithic ceramics exhibit brittleness and poor machinability, which limit their adoption into a myriad of advanced applications.[1, 2] In order to increase mechanical performance of ceramic systems, incorporating a reinforcing phase, ranging in scale from particulate to continuous fiber, into a ceramic matrix has been well investigated for a variety of ceramic matrix composite (CMC) systems.[3, 4, 5, 6] The enhanced material performance that reinforcing phases afford, due to notably improved toughening behavior, make ceramic composites attractive material systems for applications in a variety of fields, ranging from aerospace and automotive to biomedical.[7 8, 9] Although continuous fiber reinforcement lends superior mechanical improvements,[5, 10] incorporation of chopped fiber or whiskers into a number of ceramic systems offers less burdensome processing routes, coupled with notable improvements in fracture toughness and thermal shock resistance, compared with traditional monolithic systems.[11, 12]

Introducing a discontinuous reinforcing phase, like chopped fiber, into a ceramic system can be accomplished via a number of processing routes. More traditional methods involve combining ceramic powder with a discontinuous reinforcing phase, whether through wet ball or attrition milling typically in a solvent, followed by drying of the powder mixture. The resulting powder mixture can then be cold pressed into simple geometries for densification by hot pressing, pressureless sintering or spark plasma sintering [13, 14, 15] or combined with binders to enable processing by extrusion, slip casting or other colloidal processes to yield parts for sintering.[16, 17, 18, 19]

Despite relative success in producing near-net shape ceramic composites with a discontinuous reinforcing phase, attaining a high degree of alignment to maximize mechanical benefit for particular structural applications has proven a significant design hurdle in the production of complex-shaped composites, including pipes and tubes.[20] Circular pipes and tubes of varying sizes with radial reinforcement are desirable geometries for many advanced CMC applications, including shaft sleeves for slide bearings in pumps and high-performance aircraft exhaust pipes. CMC pipes and tubes are inherently difficult shapes to manufacture with a highly aligned reinforcing phase by conventional processing routes due to the manufacturing challenges associated with attaining proper dispersion of powder and chopped fiber, as well as avoiding defects, including porosity, excessive surface roughness and cracking, that could be detrimental to the mechanical performance of the component.[5, 21] Preparing slurries with high solids content leads to parts with higher packing densities, which is critical in reaching high sintered densities.[22] Consequently, optimizing chopped fiber content, while maximizing powder content in slurries necessitates use of dispersants, which often require harsh crosslinking or curing agents or solvents, in order to facilitate homogenous mixing of ceramic powder with chopped fiber to prevent powder and/or chopped fiber agglomeration while maintaining desirable flow properties. Furthermore, after processing the development of hoop stresses caused by shrinkage during drying and/or densification further complicates production of tube-shaped parts without defect or crack formation, often necessitating costly post-processing machining to achieve the desired geometry.

Previous investigations of aqueous, highly loaded ceramic suspensions have successfully produced dense near-net shape specimens of alumina, zirconium diboride, boron carbide and silicon nitride by a variety of methods, including room-temperature injection molding and additive manufacturing.[23, 24, 25, 26, 27, 28] This paper presents an environmentally benign method, referred to as Horizontal Dip Spin Casting (HDSC), as an alternative to typical processes used for short fiber CMC processing by utilizing unique ceramic-PVP suspensions[21] to produce near-net shape ceramic tube specimens with a discontinuous fiber phase. During HDSC forming, cylindrical foam molds were dipped into the aqueous suspension and rotated radially about its long axis at varying forming speeds to align thechopped fiber. A model system of alumina with chopped carbon fiber up to 30 vol.% was selected to probe rheological behavior, as well as the processability and alignment of the fiber phase under varying HDSC processing conditions. Successful completion of this model system will pave the way for more advanced and high-temperature CMC systems.

2. Experimental procedure

2.1 Materials

Suspensions that were evaluated in this study consisted of A-16 SG alumina (Almatis, New Milford, CT) with an average particle size of 0.48 ± 0.13 µm as confirmed by a Beckman Coulter LS 230 particle size analyzer (Brea, CA) and BET surface area of 7.8 ± 0.22 m^2/g determined by a TriStar 3000 gas adsorption analyzer (Micromeritics Instrument Corporation, Norcross, GA). The alumina particles were dispersed in deionized (DI) water using Dolapix CE64 (Zschimmer & Schwarz, Milledgeville, GA). Dolapix CE64 is an anionic dispersant of a poly(methacrylic acid) ammonium salt[29] that allows for high powder loadings and flowability.[23] The polymer binder introduced to modify the flow properties of the ceramic slurry was polyvinylpyrrolidone (PVP, 1-Ethenyl-2-pyrrolidinone homopolymer, Sigma-Aldrich, St. Louis, MO) with average molecular weights of 55,000 g/mol and 1,300,000 g/mol. Commercially available Panex® 35 Flake Type chopped carbon fiber (Type-13) (Zoltek, St. Louis, MO) was used as a secondary phase that would offer contrast against an alumina matrix for stereological evaluation of fiber alignment in green body specimens prepared by HDSC. The chopped C-fibers were 100-200 μm in length and nominally 7.2 μm in diameter.[30]

2.2 Suspension preparation

Alumina ceramic suspensions with chopped C-fiber were prepared by a series of steps. Initially, a slurry of DI water, dispersant and alumina powder was made by ball milling in Nalgene bottles with alumina milling media (U.S. Stoneware, East Palestine, OH) for 24h. The ceramic powder was incrementally added with dispersant and DI water to yield slurries with high alumina concentrations. A separate solution of DI water and a mixture of PVP with molecular weights of 55,000 g/mol and 1,300,000 g/mol combined in equal parts was concurrently prepared by magnetically stirring for 24 to 48h until homogenized. The ceramic slurry and PVP solution were then combined and ball milled for an additional 24h until uniformly dispersed. Previous investigations determined that 2.5 vol.% PVP yielded suspensions with suitable rheology and ultimately alumina specimens near full density with superior mechanical properties by room-temperature injection molding.[23, 24] Consequently, a similar PVP content of 2.6 vol.% was utilized in suspension preparation. The composition of all suspensions studied is shown in Table 1.

Chopped C-fiber was incrementally added to the resulting ceramic suspensions and ball milled until a dispersed suspension resulted. Chopped C-fiber loadings evaluated were 10, 20 and 30 vol.% with respect to alumina content. Corresponding alumina powder loadings were determined to be 50, 44 and 38 vol.%, respectively. A suspension of 55 vol.% alumina without chopped C-fiber was prepared as a control for HDSC processing.

2.3 Processing via Horizontal Dip Spin Casting (HDSC)

In order to prepare specimens via HDSC as shown in Figure 1(a) and (b), an ethylene propylene diene monomer (EPDM) closed-cell foam rubber tube with a firmness of 35.5 to 62.1 kPa (~5 to 9 psi) (McMaster-Carr, Elmhurst, IL) was fixed in a horizontal position on a machining lathe (parallel to the surface of the suspension) and rotated radially about its long axis. In a second step the suspension, which was placed on a small scissor platform, was brought in contact with the rotating EPDM mold. The wetting of the mold surface and the shear thinning behavior of the suspension allowed the suspension to flow around the mold and cover its exterior surface. Simultaneously, a doctor blade was set to a predetermined distance of 1.9 mm between the mold surface and the blade edge to obtain an even surface. Once the mold was entirely covered with the suspension to the desired thickness, the suspension on the scissor platform was lowered before the rotation of the mold was stopped such that the doctor blade was carefully taken out of contact with the specimen surface. After forming, the green body on the EPDM mold was left to dry at ambient conditions for six to 12 hours.

In order to optimize the HDSC process, lathe rotational speeds of 100, 200 and 300 rotations per minute (RPM) were selected. 100 RPM was identified as the lowest rotational speed due to the lathe inductor not working below that speed. Above rotational speeds of 300 RPM, suspensions were observed to not adhere readily to the EPDM foam molds. Consequently, forming speeds no higher than 300 RPM were investigated in this study. The specimens that were processed via HDSC were compared in terms of their machinability and whether cracks developed during drying. Two basic machining operations were performed on the specimens after drying to investigate machinability in the green state. First, a sanding block was set against the surface of the specimen to grind down the lip that formed during the HDSC process (refer to the highlighted area in Figure 2). The second machining operation consisted of making cross-sectional cuts of the specimens to obtain rings using the lathe with a rotational speed of 500 RPM.

2.4 Characterization

The rheological response of the suspensions containing chopped carbon fibers (compositions listed in Table 1) was evaluated using a TA Instruments ARG2 rheometer (New Castle, DE) with a 40 mm parallel plate geometry and a gap of 500 µm at 25°C with a moisture trap utilized to prevent evaporation of the suspensions. Suspensions were pre-sheared at the maximum shear rate (100 s^{-1}) for five minutes and stabilized for one minute before ramping continuously to 100 s^{-1} and back to 0 s^{-1} to obtain flow curves. The resulting flow curves were then fitted to the Herschel-Bulkley model for yield-pseudoplastic fluids[31] given by:

$\sigma = \sigma_y + k\dot{\gamma}^n$ Equation 1

where σ was stress, σ_y corresponded to the shear yield stress, k was consistency or apparent viscosity, $\dot{\gamma}$ was the applied shear rate and n, which varied from 0 to 1, represented the flow index of the suspension. When a suspension exhibited a $\sigma_y > 1$ and $n < 1$, flow behavior was determined to be yield-pseudoplastic.[31] Oscillation stress sweeps were run at a frequency of 1 Hz from 0.1 Pa to 1000 Pa, and frequency sweeps were performed at an oscillation stress of 1 Pa (in the determined linear viscoelastic region) from 0.01 to 100 Hz.

A series of experiments were conducted to quantify the effect of forming speed and chopped fiber on alignment of the fiber phase in the specimens. Because of the geometry of the specimens fabricated via HDSC, a two-dimensional approach was used to characterize the alignment of the microstructures containing C-fibers. By considering images from the tangential plane (TP) to the outer surface and the circular cross-section (CC) planes of the green body specimen (as indicated in Figure 3), an orientation descriptor, f_p, was calculated for each orientation by the following equation:[32]

$$f_p = \Delta\rho / \left\{ \Delta\rho - 4 \log \left[cos \left(\frac{\omega}{2} \right) \right] \right\} \qquad \text{Equation 2}$$

where $\Delta\rho$ and ω are the maximum and the half-width of a peak function, respectively. The peak function, as depicted in Figure 4, was calculated from the radial intensity of a Two-Dimensional Fast Fourier Transform (2DFFT) taken from a binary image. A MATLAB® routine was used to calculate the peak function from a 2DFFT for each of the images in this stereological study. Five micrographs were taken using optical microscopy of each plane shown in Figure 3 for specimens given in Table 1 at the three forming speeds to calculate an average f_p that quantified fiber deviation in orientation from the shear flow direction induced during HDSC. Values for f_p range from 0 to 1, where 1 corresponds to perfect alignment in the orientation of shear flow and 0 corresponds to a random alignment, with intermediate values corresponding to partial states of orientation.

Statistical significance of the orientation parameter data was confirmed via a two-tailed *t*-test. An *F*-test was first used on the data sets to determine if they had equal variances, which determined whether a *t*-test with equal variances (homoscedastic) or a *t*-test with unequal variances (heteroscedastic) was used. Both the *F*-test and *t*-tests were calculated using Microsoft Excel functions, and data sets were considered statistically significant if $p < 0.05$.

3. Results and Discussion

3.1 Rheological behavior of suspensions with varying C-fiber content

Flow curves of alumina-PVP suspensions containing 0, 10, 20 and 30 vol.% chopped fiber are shown in Figure 5. The flow curves of alumina-PVP suspensions containing 0, 10 and 20 vol.% chopped fiber followed a yield-pseudoplastic behavior, evidenced by their fit to the Herschel-Bulkley model with R^2 values of 0.999 or higher. Table 1 lists the Herschel-Bulkley parameters, including yield shear stress, σ_y, associated with each suspension formulation. The suspension without chopped fibers exhibited the highest yield shear stress of 114.6 Pa, while increasing fiber additions with simultaneous decrease of alumina content resulted in lower yield shear stresses ranging from 51.0 to 90.9 Pa. For suspensions containing 30 vol.% chopped fiber, the flow curve suggested suspension instability due to scatter across the shear rate range investigated. Despite the scatter, the R^2 value was 0.990 for the curve fit that yielded the Herschel-Bulkley parameters given in Table 1.

An increase in yield shear stress typically indicates flocculation within a suspension, which would be expected with an increase in solids content.[33, 34] However, because both chopped fiber and alumina contents were varied simultaneously, the difference in yield shear stress could not be solely ascribed to fiber or alumina content. Previous investigations of other ceramic-based suspensions with discontinuous phase[35, 36] have suggested that the decrease in yield shear stress could be attributed to alignment of the chopped fiber phase, allowing for easier flow of the suspension, while alumina content was simultaneously reduced to accommodate higher fiber loadings. At high chopped fiber concentrations the flow of the suspension is not as stable due to a network effect that impedes the alignment and displacement of the reinforcing phase, which requires laminar flow behavior.[37, 38] The instability in the flow of the suspension with highest fiber loading was likely caused by less efficient packing of the chopped fibers under shear flow conditions.

The viscoelastic response of the alumina-PVP suspensions with and without chopped C-fiber was investigated using oscillation stress sweeps. Figure 6 shows the storage modulus, *G'*, of the four suspensions given in Table 1 at an oscillation frequency of 1 Hz from 0.1 Pa to 1000 Pa. Consequently, all suspensions, regardless of carbon fiber and powder content, exhibited a viscoelastic behavior. Furthermore, the linear viscoelastic region was between 10 to 100 Pa for all of the suspensions, except for the suspension containing 20 vol.% fiber, which started at approximately 4 Pa. Although significant scatter was observed for suspensions without and with 30 vol.% carbon fiber at oscillation stresses below 1 Pa, these two suspensions appeared to exhibit the highest *G'* over the range investigated. The suspension with 10 vol.% chopped fiber and 49.2 vol.% alumina showed the third highest *G'* value, whereas the suspension with 20 vol.% chopped fiber and 43.7 vol.% alumina exhibited the lowest *G'* over the oscillation stress range investigated.

In order to simplify the complex modulus response, frequency sweeps at 0.01 to 100 Hz were taken at 1 Pa, which was inside the linear viscoelastic region, per the results given in Figure 6. Figures 7(a) and (b) show the storage, *G'*, and loss, *G"*, moduli for the four suspensions with and without chopped fibers and the three suspensions with chopped fibers, respectively. Data for the loss moduli of the suspension without fibers was too scattered, suggesting that the rheometer used in this study was not sensitive enough to measure the loss moduli for this particular composition. Consequently, the *G"* data for the alumina suspension was excluded. Each fiber-containing suspension exhibited *G'*>*G''*, suggesting that these suspensions demonstrated a more elastic-like behavior over the frequency range evaluated. Although *G"* data for the suspension containing 30 vol.% chopped fiber was scattered at approximately 10 Hz, which was likely the result of rheometer insensitivity, the trend of *G'*>*G"* appeared to hold for the majority of the frequency range investigated. Overall, the storage modulus decreased while the loss modulus increased with increasing chopped fiber content coupled with decreasing alumina powder amount in comparison with the suspension without chopped fiber. This behavior suggested a loss in the elastic character with the addition of carbon fiber.[39] The reduction of the elastic behavior of the suspension containing 30 vol.% chopped fiber was less pronounced than for the suspensions containing 10 and 20 vol.% chopped fiber. Consequently, the suspension with 30 vol.% chopped fiber was not as stable as the other suspensions under HDSC flow conditions, which was, again, likely due to the inability of the chopped fiber to align in order to flow and then return to a stable configuration after an applied shear stress due to the high fiber concentrations even with the lowered alumina powder content. Despite the addition of chopped fiber to the alumina suspensions, the trend in viscoelastic behavior observed was similar to that of alumina-PVP suspensions previously investigated.[23] Similarly, the suspensions investigated in this study did not exhibit a strong thixotropic response, as evidenced by a lack of a large discontinuity between the viscosity profiles taken at both increasing and decreasing applied shear rate, seen in Figure 8.

3.2 Horizontal Dip Spin Casting of alumina/chopped fiber specimens

Alumina tube-shaped specimens with 10, 20 and 30 vol.% chopped fibers were effectively prepared by Horizontal Dip Spin Casting at all forming speeds investigated. Figure 9 shows specimens prepared by suspensions with varying carbon fiber content at a forming speed of 200 RPM. The forming speed did not appear to appreciably affect the resulting exterior surface of specimens prepared with a particular suspension composition. However, suspension formulation appeared to directly impact the surface quality of a specimen after forming. Specimens prepared with suspensions containing 0 to 20 vol.% chopped fiber exhibited smooth surfaces with little roughness and/or minor defects. The surface of specimens prepared with suspensions containing chopped fiber showed an increase in surface defects resulting in visually rougher surfaces with increasing fiber content (refer to Figure 9). The quality of the surface was likely directly affected by the flow properties of the suspension when flowing under the doctor blade during processing.

The hoop stresses that likely developed during drying of the suspension on the compliant EPDM mold after HDSC were effectively minimized such that specimens without visible through-thickness cracks were successfully produced by HDSC. The formation of a lip (refer to Figure 2) that resulted from contact with the doctor blade at the conclusion of forming by HDSC was observed after processing of all suspensions investigated. By sanding the surface of the green bodies after drying using a sanding block and lathe, the lip was effectively removed from all specimens except for those prepared by suspensions containing 30 vol.% chopped fiber. The specimens in the green state prepared from the suspensions containing 30 vol.% chopped fiber tended to chip or break during the sanding step. Thus, specimens cast from suspensions containing 0, 10 and 20 vol.% carbon fiber were deemed readily machinable in the green state, whereas the green bodies prepared from suspensions of 30 vol.% chopped fiber were considered too brittle for green machining. In the second machining step, the green bodies that exhibited effective machinability by sanding were also effectively cut into cross-sections for analysis of fiber alignment.

3.3 Characterization of chopped fiber alignment in alumina specimens

The orientation parameter, f_p, was calculated using a MATLAB® routine that analyzed a micrograph, as depicted in the schematic of Figure 4, for the tangential and circular cross-section planes shown in Figure 3. Only the fibers, as opposed to the particle-like features corresponding to fibers into the particular orientation plane, contributed to the calculation of f_p. Figures 10(a) and (c) highlight the schematic corresponding to the tangential and circular cross-section planes, respectively, of the tube-shaped specimens prepared by HDSC. Figures 10(b) and (d) showing corresponding representative optical micrographs of specimens prepared from suspensions of 10 vol.% chopped fiber at a forming speed of 100 RPM in the tangential and cross-section planes, respectively. Each optical micrograph exhibited a combination of fiber orientations that appeared as point-like features and fibers with varying length in both the tangential and cross-section planes. However, optical micrographs of specimens in the longitudinal plane exhibited mostly particle-like features, as shown in Figure 11. Consequently, orientation parameters from the longitudinal cross-section plane were not calculated due to the inability of the MATLAB® routine to calculate orientation angle of these point-like features. Based on the geometry of the features observed, orientation parameters from only the tangential and cross-section planes were needed for analysis performed in this study.

Figure 12(a) and (b) shows the orientation parameters in the tangential and cross-section planes, respectively, with respect to forming speed for specimens prepared with suspensions containing 10 and 20 vol.% chopped fiber. The highest degree of chopped fiber alignment was observed in the tangential plane of specimens prepared with suspensions containing 10 vol.% chopped fiber at 100 RPM (average f_p = 0.78). Student's t-test studies indicated this value was statistically greater than the orientation parameters of the specimens prepared with the same suspensions at other speeds, while the specimens made at 200 and 300 RPM had statistically insignificant f_p values relative to each other. The average f_p in the tangential plane for specimens made with 20 vol.% chopped fiber suspensions were statistically smaller ($p \ll 0.05$ in all cases) than those made with 10 vol.% chopped fiber, ranging from 0.53 to 0.59. Even though all the orientation descriptors obtained were >0.5, degree of alignment noticeably decreased with increasing chopped fiber content in suspensions. This lower degree of alignment was attributed to the inability of the fibers to achieve alignment when flowing under the doctor blade during the HDSC process in suspensions with the higher 20 vol.% chopped fiber content.

In the circular cross-section plane, the highest degree of chopped fiber alignment was again seen in the specimens prepared from suspensions with 10 vol.% chopped fiber (average f_p = 0.68) at 300 RPM. Amongst specimens prepared from 10 vol.% chopped fiber, those produced at 100 RPM had the lowest statistical average f_p of 0.50, while the average f_p values for specimens produced at 200 and 300 RPM were statistically similar. Furthermore, the average f_p values calculated from the circular cross-section plane were statistically similar for both 10 and 20 vol.% chopped fiber specimens at 100 and 200 RPM. Overall, fiber alignment showed a smaller statistical dependence on the forming speed as compared to the suspension fiber loading. Alignment was also seen more prominently in the tangential plane as compared to the circular cross-section, as expected due to the likelihood of the highest shear stresses being at the outer diameter of the specimen (closest to the doctor blade) during forming.

The statistically higher degree of alignment of the chopped fiber phase in the tangential plane in specimens prepared by HDSC of suspensions containing 10 vol.% chopped fiber suggested that this composition yielded specimens with greater fiber alignment by HDSC, particularly at rotational speeds of 100 RPM. Despite possessing a lower yield stress, suspensions containing 20 vol.% chopped fiber had a higher flow index, indicating less pseudoplasticity, than suspensions containing 10 vol.% chopped fiber (refer to Table 1). The higher degree of shear thinning likely enhanced flowability of suspensions with 10 vol.% chopped fiber at the high shear stresses encountered during HDSC processing. The more suitable flow properties of the suspensions containing 10 vol.% chopped fiber likely facilitated greater alignment of the fibers in the HDSC specimens. Because the alignment of the chopped fiber phase was high (f_p>0.5) for all rotational speeds in both the tangential and cross-section planes, the HDSC process demonstrated promise as a novel, green approach to produce ceramic parts with an aligned discontinuous phase.

4. Summary and Conclusions

The HDSC process allowed for fabrication of tube-shaped alumina specimens with an aligned high aspect ratio phase of chopped carbon fiber utilizing aqueous alumina-PVP suspensions. Investigation of the alumina-PVP suspensions with varying chopped fiber content revealed that the flow and viscoelastic properties of suspensions containing 30 vol.% chopped fiber did not allow for stable laminar flow under the doctor blade during HDSC processing due to its inferior viscoelastic response, which resulted in specimens with excessive surface roughness. 10 and 20 vol.% fiber additions to the alumina suspensions resulted in yield-pseudoplastic behavior coupled with a highly elastic frequency response (G'>>G"), allowing for fabrication of uniform and machinable green bodies with smooth surface finishes.

The alignment of the chopped fiber in the microstructures of specimens prepared from alumina-PVP suspensions containing 10 and 20 vol.% were characterized using a 2DFFT to calculate an orientation parameter in two separate cross sections in the specimen. A high degree of alignment (f_p > 0.5) in both the tangential and cross-section planes was observed for specimens produced by HDSC, suggesting that HDSC effectively produced tube-shaped parts with a highly aligned discontinuous phase. Furthermore, specimens prepared by HDSC with suspensions containing 10 vol.% carbon fiber at rotational speeds of 100 RPM exhibited the highest degree of alignment observed in this study. The high degree of alignment was attributed to the more favorable rheological properties of the suspension under the processing conditions.

HDSC has been proven an effective method to produce tube-shaped ceramic green bodies with a highly aligned discontinuous fiber phase in this initial investigation of HDSC focused on a model material system of alumina and chopped carbon fiber. Future efforts will focus on HDSC manufacture of tube-shaped specimens of more relevant material systems for further evaluation of processability, as well as investigation of sintering and mechanical properties, to advance this unique green ceramic processing method.

5. Acknowledgements

The authors thank Prof. Alyssa Panitch and her group in the Weldon School of Biomedical Engineering at Purdue University for training and use of rheometric equipment. This work was supported by the U.S. National Science Foundation Materials and Surface Engineering Grant CMMI-0726304, the U.S. Department of Education GAANN Grant

P200A10036, Purdue University College of Engineering Bilsland Dissertation Fellowship, Army Research Office Grant W911NF-13-1-042, the National Science Foundation Graduate Research Fellowship Grant DGE-1333468 and the NASA Aeronautics Research Mission Directorate Transformational Tools and Technologies Project.

References

1. Wachtman, JB. Mechanical Properties of Ceramics. New York: John Wiley & Sons, Inc.; 1996.

2. Chiang, YM, Kingery, WD, Birnie, DP. Physical Ceramics: Principles for Ceramic Science and Engineering. New York: John Wiley & Sons, Inc.; 1997.

3. Taya, M, Hayashi, S, Kobayashi, AS, et al. Toughening of a Particulate-Reinforced Ceramic-Matrix Composite by Thermal Residual Stress. *J. Amer. Cer. Soc.* 1990; 73:1382-91.

4. Budiansky, B, Amazigo, JC, Evans, AG. Small-scale crack bridging and the fracture toughness of particulate-reinforced ceramics. *J. Mech. Phys. Solids*. 1988; 36:167-87.

5. Bansal, NP, Lamon, J. Ceramic Matrix Composites: Materials, Modeling and Technology. New York: John Wiley & Sons; 2014.

6. Krenkel, W. Ceramic Matrix Composites: Fiber Reinforced Ceramics and Their Applications. New York: John Wiley & Sons; 2008.

7. Ohnabe, H, Masaki, S, Onozuka, M, et al. Potential Application of Ceramic Matrix Composites to Aero-Engine Components. *Comp. Pt. A: Appl. Sci. Manuf.* 1999; 30:489-96.

8. Kaya, H. The Application of Ceramic Composites to the Automotive Ceramic Gas Turbine *Comp. Sci. Tech.* 1999; 58:861-72.

9. Kong, YM, Kim, S, Kim, HE, et al. Reinforcement of Hydroxyapatite Bioceramic by Addition of ZrO_2 Coated with Al_2O_3. *J. Am. Cer. Soc.* 1999; 82:2963-68.

10. Mallick, PK, Fiber-Reinforced Composites: Materials, Manufacturing, and Design. CRC press; 2007.

11. Becher, PF, Hsueh, CH, Angelini, P, et al. Toughening Behavior in Whisker-Reinforced Ceramic Matrix Composites. *J. Am. Cer. Soc.* 1988; 71:1050-61.

12. Strife, J. Status of Continuous Fiber-Reinforced Ceramic Matrix Composite Processing Technology. Ceram. Eng. Sci. Proc. 2009; 11:871-919.

13. Guicciardi, S. Silvestroni, L. Nygren, M. et al. Microstructure and Toughening Mechanisms in Spark Plasma-Sintered ZrB2 Ceramics Reinforced by SiC Whiskers or SiC-Chopped Fibers. *J. Am. Cer. Soc*. 2010; 93:2384-91.

14. Sciti, D, Silvestroni, L, Bellosi, A. High-Density Pressureless-Sintered HfC-Based Composites. *J. Am. Cer. Soc*. 2006; 89:2668-70.

15. Wang, H, Wang, CA, Yao, X, et al. Processing and Mechanical Properties of Zirconium Diboride-Based Ceramics Prepared by Spark Plasma Sintering. *J. Am. Cer. Soc*. 2007; 90:1992-97.

16. Chang-an, W, Yong, H, Hongxiang, Z. The Effect of Whisker Orientation in SiC Whisker-reinforced Si_3N_4 Ceramic Matrix Composites. *J. Eur. Cer. Soc*. 1999; 19:1903-09.

17. Zhang, Y, Li, S, Han, J, et al. Fabrication and Characterization of Random Chopped Fiber Reinforced Reaction Bonded Silicon Carbide Composite. *Cer. Int.* 2012; 38:1261-66.

18. Reed, JS. Principles of Ceramics Processing. New York: Wiley-Interscience; 1995.

19. Yang, WS, Fuso, L, Biamino, S, et al. Fabrication of Short Carbon Fibre Reinforced SiC Multilayer Composites by Tape Casting. *Cer. Int.* 2012; 38:1011-18.

20. Campbell, FC. Structural Composite Materials. West Conshohocken, PA: ASM International; 2010.

21. Mostaghaci, H. Processing of Ceramic and Metal Matrix Composites: Proceedings of the International Symposium on Advances in Processing of Ceramic and Metal Matrix Composites, Halifax, August 20-24, 1989. Elsevier Science; 2013.

22. Velamakanni, BV, Lange, FF. Effect of Interparticle Potentials and Sedimentation on Particle Packing Density of Bimodal Particle Distributions During Pressure Filtration. ," *J. Am. Cer. Soc*. 1991; 74:166-72.

23. Acosta, M, Wiesner, VL, Martinez, CJ, et al. Effect of Polyvinylpyrrolidone Additions on the Rheology of Aqueous, Highly Loaded Alumina Suspensions. *J. Am. Cer. Soc*. 2013; 96: 1372-82.

24. Wiesner, VL, Youngblood, JP, Trice, RW. Room-Temperature Injection Molding of Aqueous Alumina-Polyvinylpyrrolidone Suspensions," *J. Eur. Cer. Soc*. 2014; 34:453-63.

25. Wiesner, VL, Rueschhoff, LM, Diaz-Cano, AI, et al. Producing Dense Zirconium Diboride Components by Room-Temperature Injection Molding of Aqueous Ceramic Suspensions," *Cer. Int.* 2016; 42:2750-60.

26. Costakis, WJ, Rueschhoff, LM, Diaz-Cano, AI, et al. Additive Manufacturing of Boron Carbide via Continuous Filament Direct Ink Writing of Aqueous Ceramic Suspensions," *J. Eur. Cer. Soc*. 2016; 36:3249-56.

27. Diaz-Cano, AI, Youngblood, JP, Trice, RW. Stabilization of Highly-Loaded Boron Carbide Aqueous Suspensions. *Cer. Int.* (In press).

28. Rueschhoff, LM, Youngblood, JP, Trice, RW. Near-net Shaping of Silicon Nitride via Aqueous Room-Temperature Injection Molding and Pressureless Sintering. *Cer. Int.* (In review).

29. Zschimmer & Schwarz. Dolapix CE 64. Technical Data Sheet.

30. Zoltek. Panex® 35 Flake Type chopped fiber (Type-13). Technical Data Sheet.

31. Larson, RG. The Structure and Rheology of Complex Fluids. New York: Oxford University Press; 1999.

32. McGee SH, McCullough, R. Characterization of Fiber Orientation in Short-Fiber Composites," *J. Appl. Phys.* 1984; 55:1394-403.

33. Subbanna, MS, Pradip, Malghan, SG. Shear Yield Stress of Flocculated Alumina-Zirconia Mixed Suspensions: Effect of Solid Loading, Composition and Particle Size Distribution. *Chem. Eng. Sci*. 1998; 17:3073-19.

34. Hunter, RJ. Introduction to Modern Colloid Science. New York: Oxford Science Publications; 2003.

35. Laarz, E, Carlsson, M, Vivien, BT, et al. Colloidal Processing of Al_2O_3-Based Composites Reinforced with TiN and TiC Particulates, Whiskers and Nanoparticles," *J. Eur. Cer. Soc*. 2001; 21:1027-35.

36. Gautier, S, Champion, E, Bernache-Assollant, D, et al. Rheological Characteristics of Alumina Platelet–Hydroxyapatite Composite Suspensions," *J. Eur. Cer. Soc*. 1999; 19:469-77.

37. Farkash, M, Brandon, D. Whisker aalignment by Slip Extrusion," *Mat.Sci. Eng.: A*. 1994; 177: 269-75.

38. Bergström, L. Rheological Properties of Al_2O_3-SiC Whisker Composite Suspensions," *J. Mat. Sci.* 1996; 31:5257-70.

39. Wyss, HM, Tervoort, EV, Gauckler, LJ. Mechanics and Microstructures of Concentrated Particle Gels," *J. Am. Cer. Soc*. 2005; 88:2337-48.

List of Figures

Figure 11 (a) Schematic of longitudinal cross-section plane with corresponding optical micrographs of the longitudinal cross-section of alumina specimens with (b) 10 and (c) 20 vol.% chopped carbon fiber prepared by HDSC showing only particle-like features.

Figure 12 Orientation parameters in the a) tangential plane and b) circular cross-section plane obtained for specimens prepared at varying forming speeds with suspensions containing (■) 10 vol.% and (●) 20 vol.% chopped fibers.

List of Tables

Table 1. Compositions of alumina-PVP suspensions with varying chopped fiber content with corresponding Herschel-Bulkley curve fit parameters (R^2>0.99).

Al_2O_3 Powder Content vol.%	Chopped C-fiber Content vol.% (with respect to Al_2O_3 content)	Dispersant Content vol.%	PVP-55,000 g/mol Content vol.%	PVP-1,300,000 g/mol Content vol.%	σ_y Pa	k Pa•s^n	n
54.8	0	3.8	1.3	1.3	114.6	10.0	0.69
49.2	5.5 (10.3)	3.8	1.3	1.3	90.9	14.9	0.55
43.7	10.9 (20.6)	3.8	1.3	1.3	65.9	3.78	0.68
38.3	16.4 (30.8)	3.8	1.3	1.3	51.0	6.46	0.81

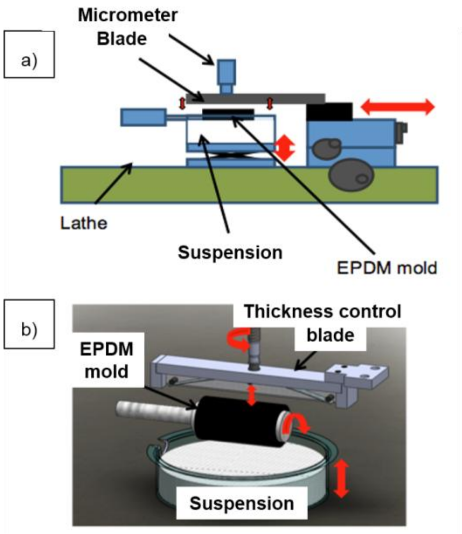
a)
Micrometer
Blade
Lathe
Suspension
EPDM mold
b)
Thickness control blade
EPDM mold
Suspension

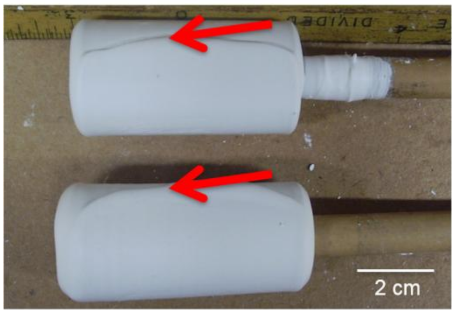
2 cm

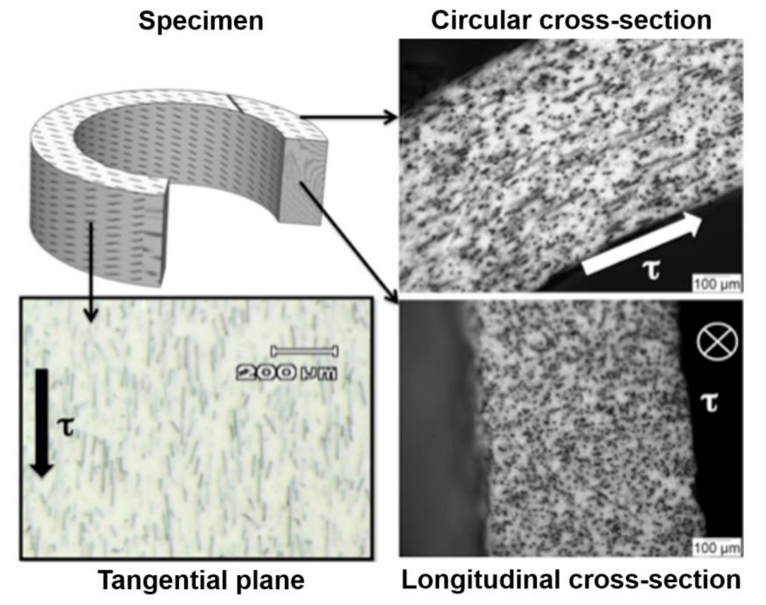
Specimen
Circular cross-section
τ
100 µm
200 µm
τ
τ
100 µm
Tangential plane
Longitudinal cross-section

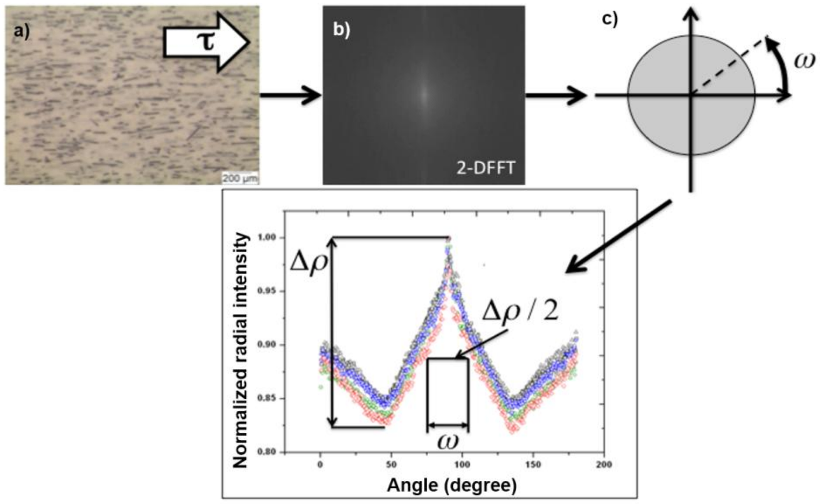
a)
τ
200 µm
b)
2-DFFT
c)
ω
Δρ
Δρ / 2
ω
Normalized radial intensity
Angle (degree)

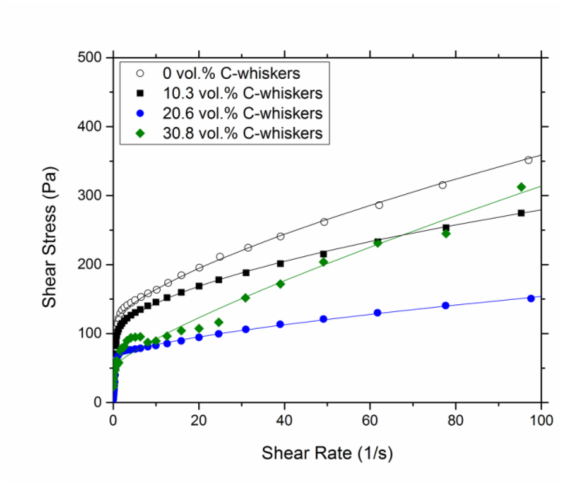

0 vol.% C-whiskers
10.3 vol.% C-whiskers
20.6 vol.% C-whiskers
30.8 vol.% C-whiskers
Shear Stress (Pa)
Shear Rate (1/s)

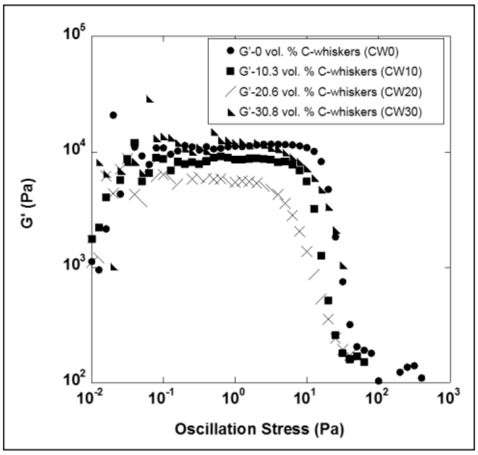

G'-0 vol. % C-whiskers (CW0)
G'-10.3 vol. % C-whiskers (CW10)
G'-20.6 vol. % C-whiskers (CW20)
G'-30.8 vol. % C-whiskers (CW30)
G' (Pa)
Oscillation Stress (Pa)

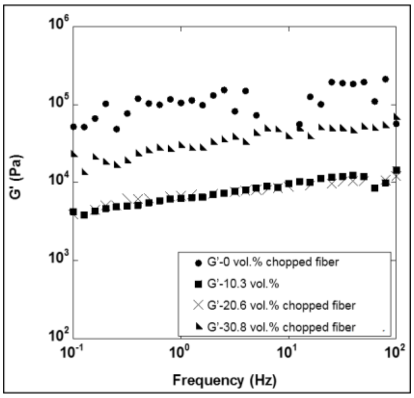
G' (Pa)
Frequency (Hz)
G'-0 vol.% chopped fiber
G'-10.3 vol.%
G'-20.6 vol.% chopped fiber
G'-30.8 vol.% chopped fiber

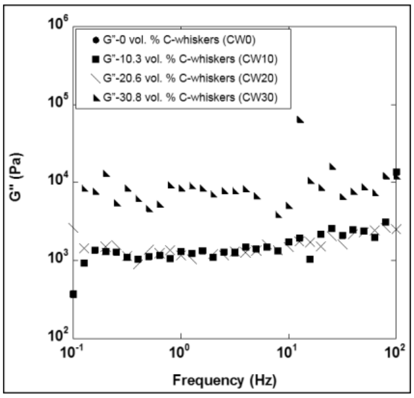
G'' (Pa)
Frequency (Hz)
G''-0 vol. % C-whiskers (CW0)
G''-10.3 vol. % C-whiskers (CW10)
G''-20.6 vol. % C-whiskers (CW20)
G''-30.8 vol. % C-whiskers (CW30)

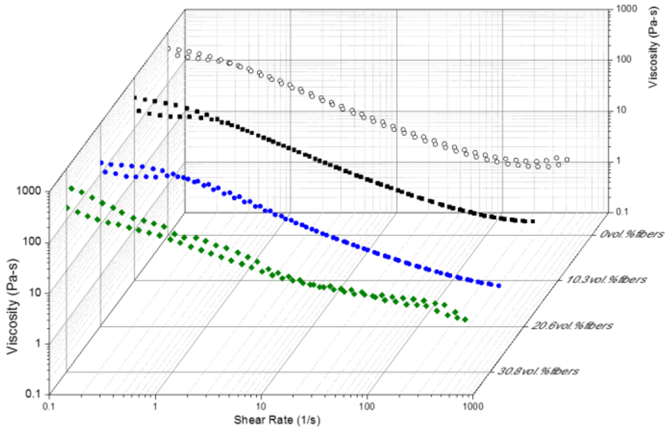
Viscosity (Pa-s)
1000
100
10
1
0.1
Shear Rate (1/s)
0.1
1
10
100
1000
0vol.% fibers
10.3vol.% fibers
20.6vol.% fibers
30.8vol.% fibers

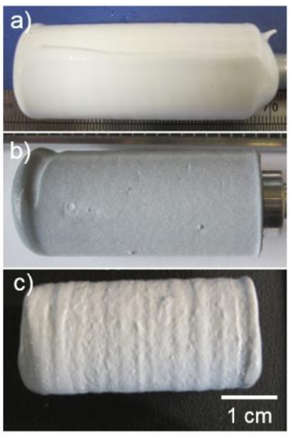
a)
b)
c)
1 cm

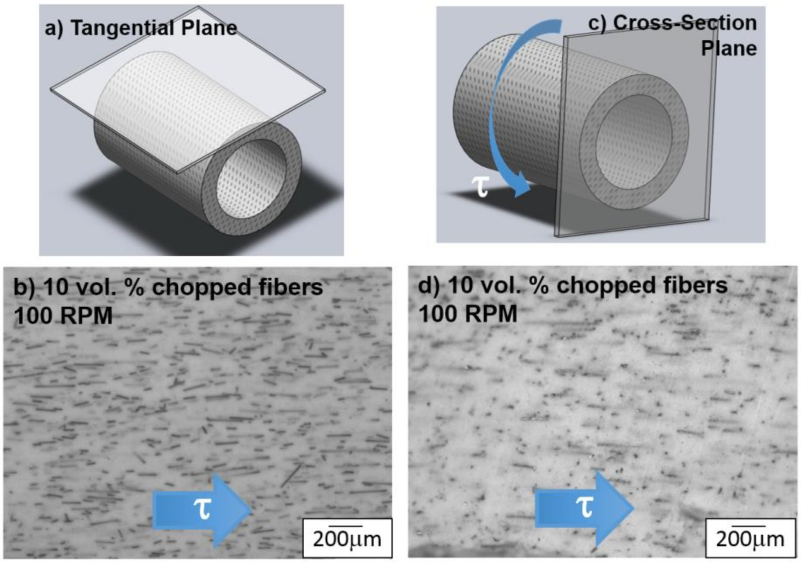
a) Tangential Plane
c) Cross-Section Plane
τ
b) 10 vol. % chopped fibers
100 RPM
τ
200μm
d) 10 vol. % chopped fibers
100 RPM
τ
200μm

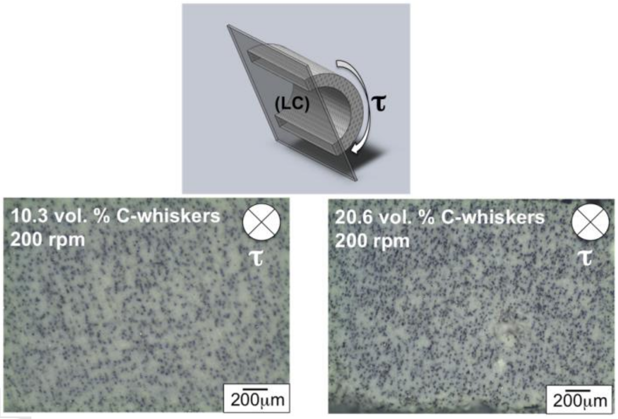
(LC)
τ
10.3 vol. % C-whiskers
200 rpm
τ
200μm
20.6 vol. % C-whiskers
200 rpm
τ
200μm

a)

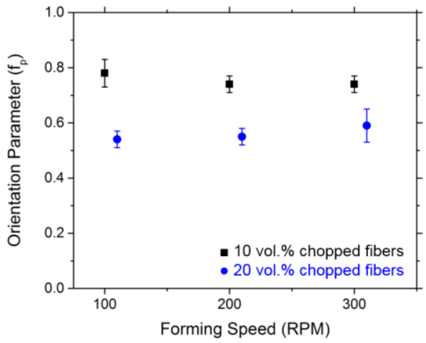
Orientation Parameter (f_p)
1.0
0.8
0.6
0.4
0.2
0.0
100
200
300
Forming Speed (RPM)
10 vol.% chopped fibers
20 vol.% chopped fibers

b)

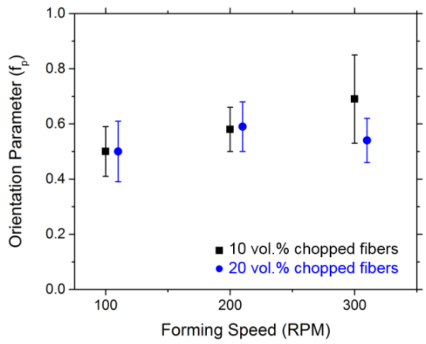
Orientation Parameter (f_p)
1.0
0.8
0.6
0.4
0.2
0.0
100
200
300
Forming Speed (RPM)
10 vol.% chopped fibers
20 vol.% chopped fibers